Applied Mathematical Sciences, Vol. 1, 2007, no. 47, 2313 - 2326

Surface Tension Effect on a Two Dimensional Channel Flow against an Inclined Wall

A. Merzougui [*], H. Mekias [**] and F. Guechi [**]

[*] Département de Mathématiques, Faculté des sciences
Université Mohamed Boudiaf, M'sila, 28000, Algérie
shamdadz@yahoo.fr

[**] Département de Mathématiques, Faculté des sciences
Université Université Farhat Abbas Sétif, 19000, Algérie

Abstract

Surface tension effect on a two dimensional channel flow against an inclined wall is considered. The flow is assumed to be steady, irrotational, inviscid and incompressible. The effect of surface tension is taken into account and the effect of gravity is neglected. Numerical solutions are obtained via series truncation procedure. The problem is solved numerically for various values of the Weber number α and for various values of the inclination angle β between the horizontal bottom and the inclined wall.

Mathematics Subject Classifications: 76B10, 76C05, 76M25

Keywords: free surface, potential flow, jet flow, Weber number, surface tension.

1. Introduction

We consider a steady two-dimensional channel flow against a wall of semi infinite length, making an angle β with the horizontal (fig.1(a)). The fluid is assumed to be inviscid, incompressible and the flow is irrotational. If we take the symmetry of the flow with respect to the bottom wall, which is a streamline, we obtain a symmetrical jet flow impinging into an angle formed by the two semi infinite plates (fig. 1(b)). Jets impinging on walls were studied by many authors.

Weidong Peng & David F. Parker [9] considered a fluid jet impinging on an uneven wall. In their article, the authors considered different smooth geometry of the wall, symmetrical and non symmetrical. Neglecting the gravity and the surface tension they could formulate the problem into an integral equation on the free boundary which they solved numerically. F. Dias, A. R. Elcrat and L. N. Trefethen [9] considered a jet emerging from a polygonal nozzle, neglecting gravity and surface tension. Despite that the problem could theoretically be solved by the hodograph and Schwartz-Christoffel transform, but in the case where the nozzle has many corners, the Schwartz-Christoffel transform is obsolete. To remedy this mathematical limitation, the authors described an efficient mathematical procedure for computing two dimensional ideal jets issuing from an arbitrary polygonal containers. J. M. Vanden-Broeck & Tuck E. O. [11] calculated flow near the intersection of a vertical wall with a free surface taking into account gravity only and then gravity and surface tension. In the later work they presented local gravity-capillary solution near the intersection of a free surface with a wall. Similar work can be found in the study of the bow flow in which the dividing streamline can be simulated to a hard bottom. In [1993] F. Dias & J. M. Vanden-Broeck [7] computed via a series truncation method a model for the spray at the bow of a ship. They considered the gravity and neglected surface tension. Because they did not neglect the gravity, the spray was modeled by a layer of water rising along the bow and following back as a jet.

In this paper we neglect the effect of gravity but we take into account the effect of surface tension. Far upstream the velocity of the flow is a constant $\widetilde{U}$ and the depth of the fluid is $\widetilde{H}$.

When the effect of surface tension and gravity g are neglected, the problem has an exact solution that can be computed via the streamline method due to Kirchhoff (see, for example [2, 3]).

If the effect of surface tension or gravity are considered, the boundary condition on the free surface is nonlinear and the problem does not have a known analytical solution. A series truncation procedure is employed to calculate the flow against a wall. This technique has been used successfully by Birkhoff and Zarantonello [3], Vanden-Broeck and Keller [12], F. Dias and Vanden-Broeck [7], to calculate nonlinear free surface flow and bow flow.

As we shall see, the flow is characterized by two parameters: the angle β between the horizontal bottom and the inclined wall, and the Weber number α defined by:

$$\alpha = \frac{\widetilde{\rho}\widetilde{U}^2\widetilde{H}}{T} \qquad 1.1$$

Here $\widetilde{T}$ is the surface tension and $\widetilde{\rho}$ is the density of the fluid.

The problem is formulated in section 2, the numerical procedure is described in section 3 and the results are discussed and presented in section 4.

2. Formulation of the problem

Let us consider the motion of a two-dimensional flow in a channel against an inclined wall of semi infinite length. the inclined wall meets the horizontal bottom at the point O making an angle β . We assume that the fluid is inviscid, incompressible and the flow is irrotational and steady. Far upstream, we assume that the velocity approaches a constant $\widetilde{U}$ and the depth of the fluid tends to a constant $\widetilde{H}$. The flow is limited by the free streamline $A'C'B'$, the horizontal bottom wall AO and the inclined wall OB. In the absence of gravity the main flow extends to infinity in the direction of the bottom wall far upstream and in the direction of the inclined wall OB far downstream (Figure 1(a)). If we take the symmetry of the flow with respect to the straight streamline AO, we obtain a symmetrical jet flow against two inclined walls making between them an angle of $2(\pi-\beta)$ (fig.1(b)). Thus, the following formulation is valid for the two problems. Our formulation is made for the flow in the channel. We choose the Cartesian coordinates such that the $\widetilde{x}-$axis is along the bottom streamline and passes through the stagnation point O and the $\widetilde{y}-$axis is vertically upward through the point O (considered as the origin of the axes). The angle β is counted positive in the counterclockwise from the positive axes. Since the flow is potential and considered to be steady with the same velocity $\widetilde{U}$ far upstream and downstream, it should be symmetrical with respect to the bisector of the angle AOB . Let C' denotes the intersection of the bisector of the angle AOB and the free surface, and let $(\widetilde{x}_c, \widetilde{y}_c)$ be its coordinates.

In this article, we neglect the effect of gravity but we take into account the effect of surface tension. if we neglect the effect of surface tension and gravity the problem has an exact analytical solution that can be computed via hodograph transformation and free streamline theory.

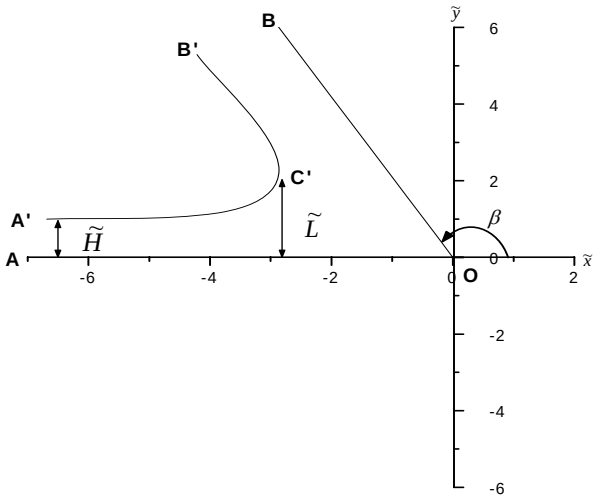

Figure 1(a). Sketch of the channel flow and the coordinates system. The depth of the flow far downstream $\widetilde{H}$. The x axis is along the bottom wall AO and the y axis is verticaly upward through the point O. The figure is an actual computed surface profile for $\beta = 2\pi/3$ and the Weber number α=200.

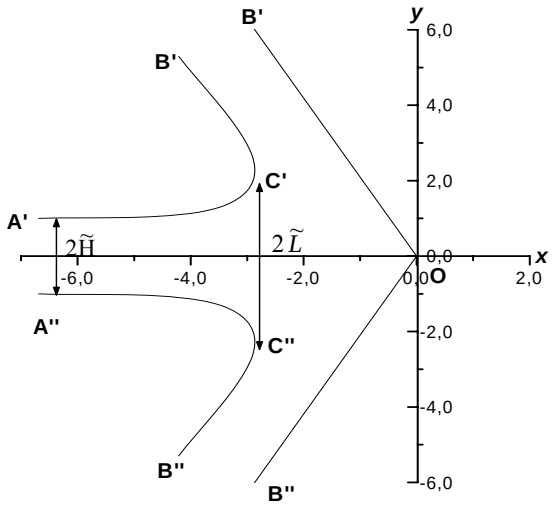

Figure 1(b). Sketch of a jet flow impinging into an angle of $2(\pi - \beta)$). The width of the jet at infinity is. The x axis is along the streamline AO and the y axis is verticaly upward through the point O. The figure is an actual computed surface profile for and the Weber number α =200.

Since the flow is irrotational and the fluid is incompressible, we define the complex variable $\tilde{z} = \tilde{x} + i\tilde{y}$ and the complex potential function $\tilde{f} = \tilde{\phi} + i\tilde{\psi}$ where $\tilde{\phi}$ is the potential function is and $\tilde{\psi}$ is the stream function. Since $\tilde{\phi}$ and $\tilde{\psi}$ are conjugate solutions of Laplace's equation, $\tilde{f}(\tilde{z})$ is an analytic function of $\tilde{z}$ within the flow region. The complex conjugate velocity is given by

$$\tilde{\zeta} = \frac{d\tilde{f}}{d\tilde{z}} = \tilde{u}(\tilde{x},\tilde{y}) - \tilde{v}(\tilde{x},\tilde{y}) \tag{2.1}$$

where $\tilde{u}$ and $\tilde{v}$ are the horizontal and vertical components of the fluid velocity, respectively, and may be expressed as

$$\tilde{u} = \frac{d\tilde{\phi}}{d\tilde{x}} = \frac{d\tilde{\psi}}{d\tilde{y}}, \qquad \tilde{v} = \frac{d\tilde{\phi}}{d\tilde{y}} = -\frac{d\tilde{\psi}}{d\tilde{x}} \tag{2.2}$$

Without loss of generality, we choose $\tilde{\psi} = 0$ on the streamline AOB and $\tilde{\phi} = 0$ at the origin O ($(\tilde{x},\tilde{y}) = (0,0)$). The complex potential $\tilde{f}$ maps the flow domain conformally onto the infinite strip of width $\tilde{U}\tilde{H}$ as shown in fig. 2.

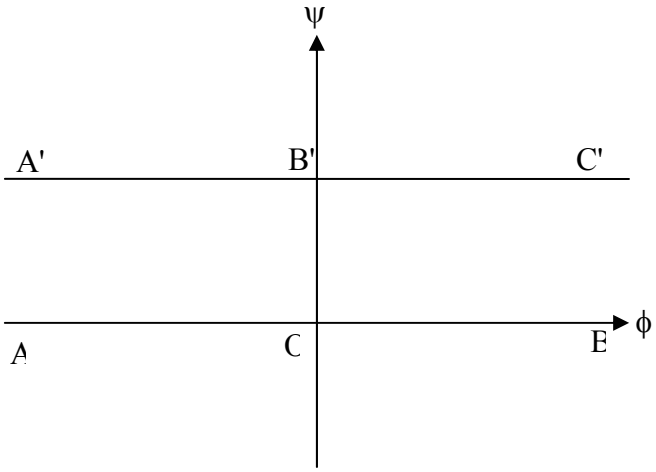

Figure 2. The complex potential plane, $\tilde{f} = \tilde{\phi} + i\tilde{\psi}$

On the free streamline (free surface) $A'C'B'$, the Bernoulli equation is to be satisfied, that is

$$\frac{1}{2}\tilde{q}^2 + \frac{\tilde{p}}{\tilde{q}} = C \quad on \quad \tilde{\psi} = \tilde{U}\tilde{H}, \quad -\infty < \tilde{\phi} < +\infty \tag{2.3}$$

where $\widetilde{p}$ is the pressure of the fluid in a point on the free surface $A'C'B'$, $\widetilde{\rho}$ is the density of the fluid and $\widetilde{q} = \sqrt{\widetilde{u}^2 + \widetilde{v}^2}$ is the speed of the fluid particle on the free surface. Let $\widetilde{p}_0$ be the pressure outside the fluid just above the free surface. $\widetilde{p}_0$ is considered to be a constant. Since far upstream the free surface is horizontal, we have $\widetilde{p} = \widetilde{p}_0$ Thus, the constant C in equation (2.3) is evaluated far upstream and is given by

$$\frac{1}{2}\widetilde{U}^2 + \frac{\widetilde{p}_0}{\widetilde{\rho}} = C.$$

A relationship between $\widetilde{p}$ and $\widetilde{p}_0$ is given by Laplace's capillary formula

$$\widetilde{p} - \widetilde{p}_0 = \widetilde{T}\widetilde{K} \tag{2.4}$$

Here $\widetilde{K}$ is the curvature of the free surface and $\widetilde{T}$ the surface tension. If we substitute (2.4) into (2.3) we obtain:

$$\frac{1}{2}\widetilde{q}^2 - \frac{\widetilde{T}}{\widetilde{\rho}}\widetilde{K} = \frac{1}{2}\widetilde{U}^2. \tag{2.5}$$

We introduce the dimensionless variables by taking $\widetilde{H}$ as the unit length and $\widetilde{U}$ as the unit velocity. The dimensionless variables are given by:

$$x = \frac{\widetilde{x}}{\widetilde{H}}; \qquad x = \frac{\widetilde{y}}{\widetilde{H}}; \qquad q = \frac{\widetilde{q}}{\widetilde{U}}; \qquad K = \frac{\widetilde{y}}{\widetilde{R}}; \qquad c = \frac{\widetilde{y}_c}{\widetilde{H}}. \tag{2.6}$$

the dimensionless parameter c has a special characteristic: it measures the ratio of the depth of the nearest point on the free surface to the stagnation point O to the depth of the fluid at infinity, in some literature this ratio is called the contraction coefficient. The free surface condition (2.5) reduces to

$$q^2 - \frac{2}{\alpha}K = 1 \tag{2.7}$$

Here α is the Weber number defined in (1.1).
We rewrite the dimensionless complex velocity in the new variables τ and θ as

$$\zeta = u - iv = e^{\tau - i\theta} \tag{2.8}$$

where $e^{\tau} = |\zeta|$ and $\theta = -\arg(\zeta)$

In the new variables τ and θ (2.7) becomes

$$\frac{\partial\theta}{\partial\phi}=\frac{\alpha}{2}(e^{\tau}-e^{-\tau}) \quad \psi=1, \quad -\infty<\phi<+\infty. \tag{2.9}$$

The kinematic condition on AO and OB yields

$$\begin{cases}\theta=0, & \psi=0, & -\infty<\phi<0 & AO\\ \theta=0, & \psi=0, & 0<\phi<+\infty & OB\end{cases}. \tag{2.10}$$

We shall seek $\tau-i\theta$ as an analytic function of $f=\phi+i\psi$ in the region $0<\psi<1$. Using the shwartz-christoffel transformation, we map the strip $0<\psi<1$ in the *f*-plane onto the lower-half of the unit disk of the auxiliary *t*-plane by the transformation

$$f=\frac{2}{\pi}\log\left(\frac{1-t}{1+t}\right). \tag{2.11}$$

The stagnation point O is mapped into the origin, the points at infinity $A=A'$ and $B=B'$ correspond to the points $t=1$ and $t=-1$ respectively. Due to the symmetry, the point C is mapped onto the point $t=-i$. The solid boundary maps onto the real diameter and the free surface onto the lower half-unit circle (fig. 3).

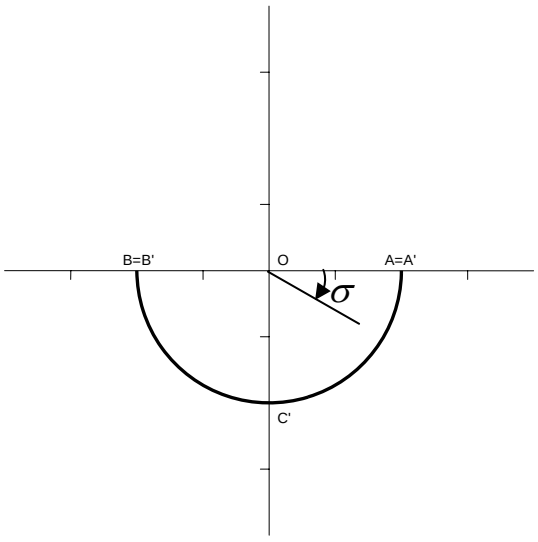

Figure 3. The complex potential t plane.

In all the flow domain, the complex velocity $\zeta(t) = u - iv$ is analytic except at the point O, which correspond to $t = 0$, where the flow is inside a corner. Hence, a close study in the neighborhood of this point is to be done.
At $t = 0$, we have a flow inside an angle of measure $\pi - \beta$, this gives the local behavior of $\zeta(t)$ as

$$\zeta = O(t^{\frac{\beta}{\pi}}) \quad as \quad t \to 0. \tag{2.12}$$

Now that we know the local behavior of $\zeta(t)$ near the singularity, we seek the function $\zeta(t)$ as a series of the form

$$\zeta(t) = t^{\frac{\beta}{\pi}} \exp(\sum_{n=0}^{\infty} a_n t^{2n}) \tag{2.13}$$

The coefficients a_n are to be determined. Since (2.13) satisfies (2.12) we expect the series to converge in the lower half disk in the *t*-plane. The coefficients a_n are chosen to be real, so that the boundary conditions (2.10) are satisfied i.e. $u = \cos\beta$ on OB and $v = 0$ on AO.
We use the notation $t = |t| e^{i\sigma}$ so that the points on $A'C'B'$ are given by $t = e^{i\sigma}$ and $-\pi < \sigma < 0$. Using (2.11) the expression (2.9) is rewritten as

$$\exp(2\tau) - \frac{\pi}{\alpha} \exp(\tau) \sin(\sigma) \left| \frac{\partial \theta}{\partial \sigma} \right| = 1 \tag{2.14}$$

3. Numerical procedure

We solve the problem by truncating the infinite series in (2.13) after N terms. Introducing the N mesh points

$$\sigma_I = -\frac{\pi}{N}(I - \frac{1}{2}), \qquad I = 1, \cdots, N \tag{3.1}$$

The N coefficients a_n are found by collocation. Using (2.14) we obtain $\tau(\sigma), \theta(\sigma)$ and $\frac{\partial \theta}{\partial \sigma}$ in terms of coefficients a_n. Upon substituting these expressions into (2.14) we obtain N nonlinear algebraic equations for the N unknowns $\{a_n\}_{n=1}^{N}$. The Weber number α and the angle β are parameters. We solve this system by Newton method for given values of α and β.

To draw the free surface we use the identity

$$\frac{\partial x}{\partial \phi}+i\frac{\partial y}{\partial \phi}=\frac{1}{\zeta}=\frac{1}{u-iv}=e^{-\tau+i\theta}. \qquad 3.2$$

In the new variables σ and τ, (3.2) rewrites

$$\begin{cases}\dfrac{\partial x}{\partial \sigma}=\dfrac{2}{\pi}\exp(-\tau)\cos(\theta)\dfrac{1}{\sin(\sigma)}\\ \dfrac{\partial y}{\partial \sigma}=\dfrac{2}{\pi}\exp(-\tau)\sin(\theta)\dfrac{1}{\sin(\sigma)}\end{cases} \qquad 3.3$$

To obtain the form of the free surface $A'C'B'$, we take advantage of the symmetry with respect to the bisector of the angle AOB. We integrate numerically the expression (3.3) in the interval $-\frac{\pi}{2}<\sigma<0,$ letting $y(N+1)$ and $x(N+1)$ be the coordinates of the point C'. With some algebra, we can find the relation $x(N+1)=\frac{y(N+1)}{\tan(\frac{\pi+\beta}{2})}$. The Euler method was used to integrate numerically the relation (3.3).

4. Results and discussion

We use the numerical procedure described in section 3 to compute solutions of the problem for various values of the Weber number α. For fixed values of α $(0<\alpha<\infty)$ and β $(0\le\beta<\pi)$ the coefficients a_n were found to decrease very rapidly as n increases (table 1).

β	α	a_1	a_5	a_{20}	a_{50}
$\frac{\pi}{4}$	0.135	-0.8505	2.0816×10^{-2}	1.7697×10^{-3}	1.8227×10^{-5}
	10	-2.3879×10^{-2}	8.7610×10^{-4}	4.0002×10^{-5}	4.1985×10^{-7}
	$\alpha \to \infty$	-4.004×10^{-21}	6.2777×10^{-21}	4.0326×10^{-21}	1.0547×10^{-21}
$\frac{\pi}{3}$	2×10^{-3}	-5.1231	2.9453×10^{-2}	2.5526×10^{-3}	2.6324×10^{-5}
	10	-3.1835×10^{-2}	1.1681×10^{-3}	5.3336×10^{-5}	5.5867×10^{-7}
	$\alpha \to \infty$	-4.004×10^{-21}	6.2777×10^{-21}	4.0326×10^{-21}	1.0547×10^{-21}
$\frac{2\pi}{3}$	3×10^{-4}	-7.6264	4.8419×10^{-2}	4.1284×10^{-3}	4.2636×10^{-5}
	10	-6.3624×10^{-2}	2.3362×10^{-3}	1.0666×10^{-4}	1.1074×10^{-6}
	$\alpha \to \infty$	-4.004×10^{-21}	6.2777×10^{-21}	4.0326×10^{-21}	1.0547×10^{-21}
$\frac{3\pi}{4}$	2×10^{-5}	-10.2719	5.2193×10^{-2}	4.4389×10^{-3}	4.5798×10^{-5}
	10	-7.1559×10^{-2}	2.6283×10^{-3}	1.1999×10^{-4}	1.2429×10^{-6}
	$\alpha \to \infty$	-4.004×10^{-21}	6.2777×10^{-21}	4.0326×10^{-21}	1.0547×10^{-21}

Table 1: Some Values of coefficients a_n of the series (2.13) for different values of the Weber number α and for different values of the angle of inclinaison β.

β	α	a_1	a_5	a_{10}	a_{30}	a_{45}
$\frac{\pi}{4}$	100	-2.4877×10^{-3}	8.0240×10^{-5}	1.5586×10^{-5}	1.2429×10^{-6}	2.4220×10^{-7}
	200	-1.2469×10^{-3}	3.9849×10^{-5}	7.7141×10^{-6}	6.1363×10^{-7}	1.1983×10^{-7}
	1000	-2.49882×10^{-4}	7.9269×10^{-6}	1.5300×10^{-6}	1.2146×10^{-7}	2.3986×10^{-8}
$\frac{\pi}{3}$	100	-3.3170×10^{-3}	1.0698×10^{-4}	2.0781×10^{-5}	1.6573×10^{-6}	3.2294×10^{-7}
	200	-1.6625×10^{-3}	5.3132×10^{-5}	1.0285×10^{-5}	8.1818×10^{-7}	1.5977×10^{-7}
	1000	-3.3317×10^{-4}	1.0569×10^{-5}	2.0400×10^{-6}	1.6195×10^{-7}	3.1981×10^{-8}
$\frac{\pi}{2}$	100	-4.9754×10^{-3}	1.6048×10^{-4}	3.1172×10^{-5}	2.4859×10^{-6}	4.8441×10^{-7}
	200	-2.4938×10^{-3}	7.9698×10^{-5}	1.5428×10^{-5}	1.2272×10^{-6}	2.3966×10^{-7}
	1000	-4.9976×10^{-4}	1.5853×10^{-5}	3.0601×10^{-6}	2.4293×10^{-7}	4.7972×10^{-8}
$\frac{2\pi}{3}$	100	-6.6339×10^{-3}	2.1397×10^{-4}	4.1562×10^{-5}	3.3146×10^{-6}	6.4589×10^{-7}
	200	-3.3250×10^{-3}	1.0626×10^{-4}	2.0571×10^{-5}	1.6363×10^{-6}	3.1955×10^{-7}
	1000	-6.6635×10^{-4}	2.1138×10^{-5}	4.0801×10^{-6}	3.2391×10^{-7}	6.3963×10^{-8}

Table 2: Some Values of coefficients a_n of the series (2.13) for different values of the Weber number $\alpha \geq 100$ and for different values of the angle of inclinaison β.

For values of α very large, ($\alpha \geq 10^2$) (table 2), all the coefficient of the series (2.13) are zeros ($a_i = 0$ for all $i \geq 1$) . This gives the exact solution for $(\alpha \to \infty)$ $\zeta(t) = t^{\frac{\beta}{\pi}}$. This result was compared with the exact solution found via

the hodograph transform due to kirchhoff and were found to agree exactly. In figure 4, the exact solution via the hodograph transform for $\beta = \frac{\pi}{2}$,

$$\begin{cases} x(s) = -1 - \frac{1}{\pi}\log\left(\frac{1+\sqrt{1-s}}{1-\sqrt{1-s}}\right) \\ y(s) = 1 + \frac{1}{\pi}\log\left(\frac{1+\sqrt{s}}{1-\sqrt{s}}\right) \end{cases} \qquad 4.1$$

was compared with the solution $\zeta(t) = \sqrt{t}$. The two solutions were found to be identical.

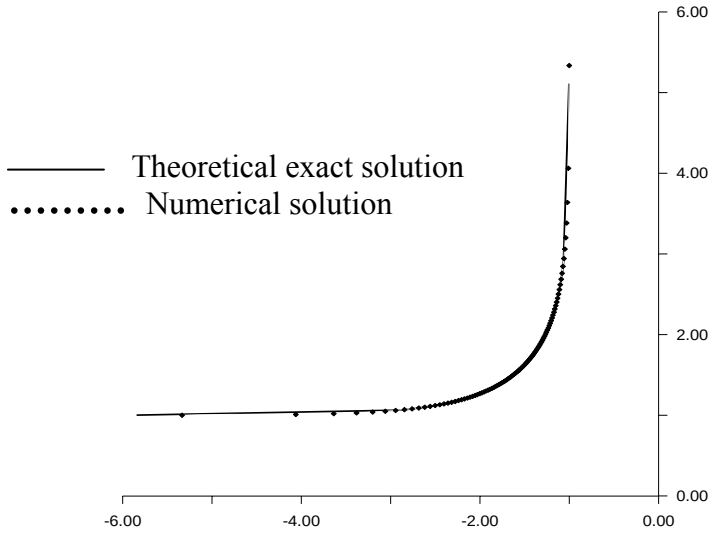

Figure 4. Comparaison of the numerical free streamline shape for $\beta = \frac{\pi}{2}$ with the exact theoretical results

With this numerical procedure we could compute solution for the Weber number α very small. As an example for $\beta = \frac{\pi}{4}$, we could compute the solution for all $\alpha \geq 0.13698$. There exists a critical value α^* (α^* very small) of α such that for $\alpha < \alpha^*$ the numerical scheme ceases to converge (table 3).

β	$\frac{\pi}{4}$	$\frac{\pi}{3}$	$\frac{\pi}{2}$	$\frac{2\pi}{3}$	$\frac{3\pi}{4}$
α^*	0.13698	0.001825	0.000605	0.00037	0.0000302

Table 3: Values of the minimal Weber number α* for different values of the angle of inclinaison β.

The free surface was smooth with no capillary waves even for small α. For each fixed β and as the Weber number decreases from ∞ to α^*, the shape of the free surface flattens and tends to a straight line (figs.5, 6 and 7).
Figure 8 shows the variation of contraction coefficient versus the Weber number α. From the above numerical results, we conclude that for a fixed value of β $(0 \le \beta < \pi)$ there exist a unique solution with no capillary surface wave for all $\alpha \ge \alpha^*$. For a fixed value of β $(0 \le \beta < \pi)$ and a given $\alpha < \alpha^*$ we conjecture that a solution exists with capillary surface wave. The later conjectured solution may be computed via an integro-differential equation which is an appropriate method for surface waves.

The results presented here are obtained with $N = 50$

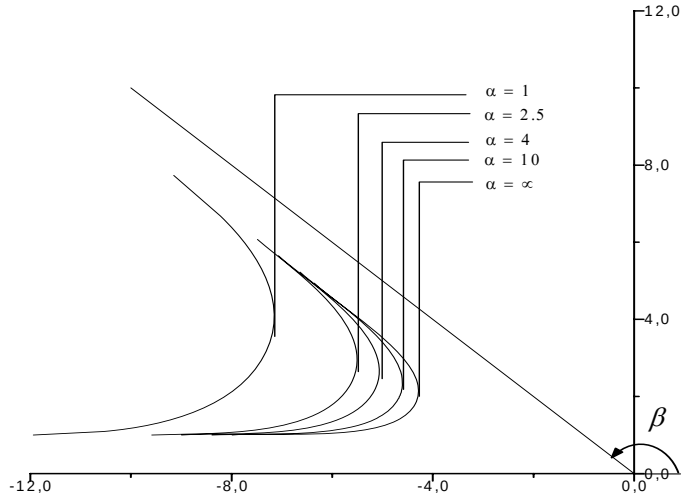

Figure 5: Free streamline shapes for $\beta = \frac{3\pi}{4}$ and various Weber numbers

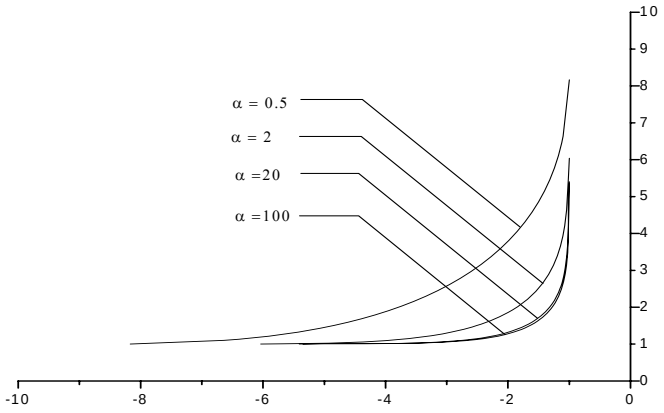

Figure 6: Free streamline shapes for $\beta=\frac{\pi}{2}$ and various Weber numbers

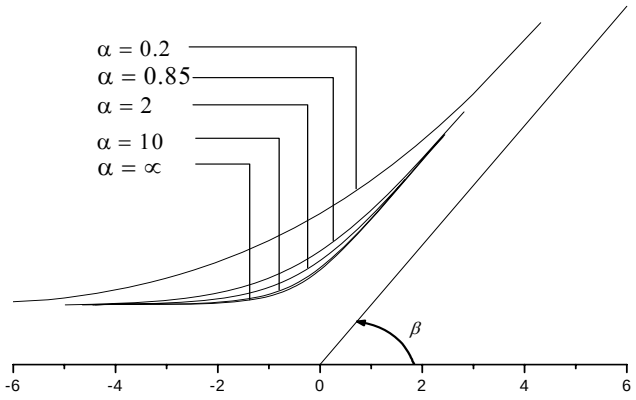

Figure 7: Free streamline shapes for $\beta=\frac{\pi}{4}$ and various Weber numbers

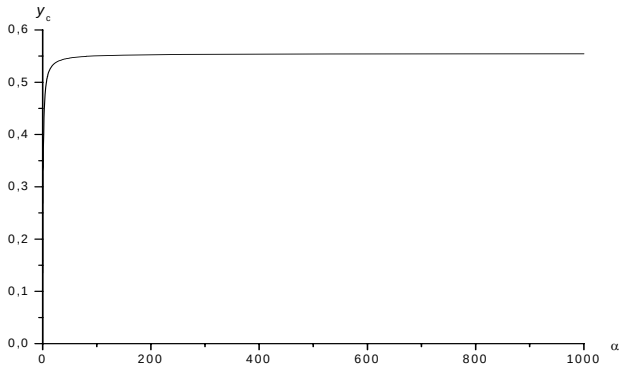

Figure 8: Coordinate y_c of the point C' versus α for $\beta = \frac{3\pi}{4}$

References

C. Andersson, J.M. Vanden Broeck, Bow flows with surface tension Proc. Roy. Soc. Lond. SER. A 452 (1996) pp 1-14.

G. K. Batchelor 1967 An introduction to fluid dynamics (Cambridge: Cambridge university press).

G. Birkhoff, E. H. Zarantonello Jets, wakes and cavities, Academic press inc New York 1957.

J.M. Chuang, Numerical studies on non linear free surface flow using generalized Schwarz-Christoffel transformation Int. J. Numer. Meth. Fluids 2000; 32:745-772.

D. Daboussy, F. Dias, J. M. Vanden Broeck, Gravity flows with a free surface of finite extent Eur. J. Mech. B/Fluids (1998) 17, n ¬ 1, pp. 19-31.

F. Dias, A. R. Elcrat and L. N. Trefethen, Ideal jet flow in two dimensions J. Fluid Mech (1987), vol 185, pp. 275-288.

F. Dias, J.M. Vanden Broeck, Nonlinear bow flow with spray J. Fluid Mech (1993), vol 255, pp. 91-102.

S. N. Hanna, M.N. Abdelmalek, M. B. Abd el malek, Super-critical free surface flow over a trapezoidal obstacle Journal of computational and applied mathematics 66, (1996), 279-291.

W. Peng, D. F. Parker An ideal fluid jet impinging on an uneven wall J. Fluid Mech (1997), vol 333, pp. 231-255.

J.M. Vanden Broeck, The effect of surface tension on the shape of the Kirchhoff jet, Phys. Fluids, 27 (1984), pp. 1933-1936.

J.M. Vanden Broeck, E.O. Tuck (1994) Flow near the intersection of the free surface with a vertical wall. SIAM J. Appl. Math. 54, 1-13.

J.M. Vanden Broeck, J.B. Keller, Weir flow, J. Fluid Mech. 176 (1987) 283-293.

J.M. Vanden Broeck, Cavitating flow of a fluid with surface tension past a circular cylinder, Phys. Fluids. A3 (1991), pp. 263-266.

Received: March 18, 2007